Development 129, 3597-3608 (2002)
Printed in Great Britain © The Company of Biologists Limited 2002
DEV4626

Mixl1 is required for axial mesendoderm morphogenesis and patterning in the murine embryo

Adam H. Hart[1], Lynne Hartley[1], Koula Sourris[1,†], Elizabeth S. Stadler[1,†], Ruili Li[1], Edouard G. Stanley[1,†], Patrick P. L. Tam[2], Andrew G. Elefanty[1,*,†] and Lorraine Robb[1,*,‡]

[1]The Walter and Eliza Hall Institute of Medical Research, P.O. Royal Melbourne Hospital, Vic 3050, Australia
[2]Embryology Unit, Childrens' Medical Research Institute, Wentworthville, NSW 2145, Australia
*These authors contributed equally to this work
†Present address: Centre for Early Human Development, Monash Institute of Reproduction and Development, 27-31 Wright St, Clayton, Vic 3168, Australia
‡Author for correspondence (e-mail: robb@wehi.edu.au)

Accepted 30 April 2002

SUMMARY

In *Xenopus*, the Mix/Bix family of homeobox genes has been implicated in mesendoderm development. *Mixl1* is the only known murine member of this family. To examine the role of *Mixl1* in murine embryogenesis, we used gene targeting to create mice bearing a null mutation of *Mixl1*. Homozygous *Mixl1* mutant embryos can be distinguished from their littermates by a marked thickening of the primitive streak. By the early somite stage, embryonic development is arrested, with the formation of abnormal head folds, foreshortened body axis, absence of heart tube and gut, deficient paraxial mesoderm, and an enlarged midline tissue mass that replaces the notochord. Development of extra-embryonic structures is generally normal except that the allantois is often disproportionately large for the size of the mutant embryo. In chimeras, *Mixl1*$^{-/-}$ mutant cells can contribute to all embryonic structures, with the exception of the hindgut, suggesting that *Mixl1* activity is most crucial for endodermal differentiation. *Mixl1* is therefore required for the morphogenesis of axial mesoderm, the heart and the gut during embryogenesis.

Key words: Mix, Bix, Homeobox, Gastrulation, Mesendoderm, Notochord, Node, Endoderm, Mouse

INTRODUCTION

In *Xenopus*, members of the Mix/Bix family of *Paired*-like homeobox genes have been implicated as regulators of gastrulation. *Mix.1*, the founding member of this family, was originally identified as an immediate-early response gene to activin induction and was later rediscovered during a screen for ventralizing molecules (Rosa, 1989; Mead et al., 1996). Currently, there are seven family members: *Mix.1*, *Mix.2*, *Mix.3*/*Mixer*, *Bix1*/*Mix4*, *Bix2*/*Milk*, *Bix3* and *Bix4* (Rosa, 1989; Vize, 1996; Ecochard et al., 1998; Henry and Melton, 1998; Mead et al., 1998; Tada et al., 1998). Transcription of all the members of the Mix/Bix family begins soon after the mid-blastula transition in presumptive mesendoderm in the equatorial region of the embryo and ceases after gastrulation. Expression requires maternal *VegT*, a T-box transcription factor that induces the *Xenopus* transforming growth factor (TGF) β-like molecules *Xnr1*, *Xnr2*, *Xnr4* and *derriere* (Xanthos et al., 2001).

Studies of MIX/BIX homeoprotein function in *Xenopus* have shown that they are downstream transcriptional targets in the TGFβ superfamily pathway that regulates mesendodermal patterning. For *Mix.2*, the pathway of activin-induced transcriptional activation has been determined. Signals from TGFβ family members are transduced to the nucleus by intracellular SMAD proteins. SMAD proteins are recruited to DNA by other DNA-binding proteins, the prototype of which is FOXH1 (FAST1). FOXH1 forms a complex with activated SMAD2/SMAD4 dimers to bind to the activin-responsive element of the *Mix.2* promoter (reviewed by Massague and Wotton, 2000). Other *Xenopus* MIX/BIX proteins, MIXER, BIX2/MILK and BIX3, recruit active SMAD2/SMAD4 complexes directly to an activin-response element found in mesendodermal genes such as *Gsc* (Germain et al., 2000).

Mix.1 has been implicated in endoderm development (Hudson et al., 1997; Lemaire et al., 1998; Latinkic and Smith, 1999). Expression of dominant negative *Mix.1* constructs prevents endoderm formation and, while overexpression of *Mix.1* does not induce endoderm formation in animal cap explants, it can act synergistically with the *Paired*-like homeobox genes *Gsc* or *Siamois* to upregulate transcription of endodermal markers (Henry and Melton, 1998; Lemaire et al., 1998; Latinkic and Smith, 1999). Moreover, *Mix.1* has been shown to repress the expression of the mesodermal marker *Xbra*, the *Xenopus* homolog of *Brachyury* (Latinkic et al., 1997; Latinkic and Smith, 1999). *Bix2*/*Milk*, *Mix.3*/*Mixer* and *Bix4* have also been shown to induce endoderm formation (Ecochard et al., 1998; Henry and Melton, 1998; Casey et al., 1999). Depending on the level of overexpression, *Bix1*/*Mix4* can induce the expression of endoderm or ventral mesoderm

markers in animal cap explants (Tada et al., 1998). However, the roles of individual Mix/Bix genes in the regulation of mesendodermal patterning in *Xenopus* remain unclear, especially as homeobox proteins are known to homo- or heterodimerize with DNA (Wilson et al., 1993; Wilson et al., 1995a; Mead et al., 1998).

In the chick, a *Mix*-like gene (*Cmix*) is expressed in epiblast and endoderm of the posterior marginal zone prior to formation of the primitive streak. Thereafter, expression is seen in epiblast and nascent mesoderm of the primitive streak but not in Hensen's node. *Cmix* transcripts are no longer detectable after formation of the head process (Peale et al., 1998; Stein et al., 1998). In zebrafish, the gene associated with the *bonnie and clyde* (*Bon*) mutation is a *Mix*-type gene with similarity to *Xenopus Mixer* (Kikuchi et al., 2000). *Bon* is induced in the margin of late blastula stage embryos by NODAL signaling and is required for early endoderm formation and, like *Mixer* in *Xenopus*, regulates expression of the endodermal gene *Sox17* (Henry and Melton, 1998; Alexander and Stainer, 1999). *Bon* mutants exhibit cardia bifida and have fewer *Sox17*-expressing endodermal cells (Alexander et al., 1999; Kikuchi et al., 2000). Genetic studies have shown that *Bon* lies downstream of the NODAL-related proteins encoded by the *Cyclops* and *Squint* genes (Kikuchi et al., 2000).

To date, one murine *Mix*-like gene, *Mixl1* (*Mml*, *Mix*) (Pearce and Evans, 1999; Robb et al., 2000) and one human homolog (Robb et al., 2000) have been identified. The amino acid sequence of the homeodomain and a conserved C-terminal acidic region of the murine MIXL1 is similar to MIX.1 and other proteins of *Xenopus* MIX/BIX family (Pearce and Evans, 1999; Robb et al., 2000). *Mixl1* RNA was first detected in the visceral endoderm of the pre-gastrula embryo. By 6.5 days post coitum (dpc), expression was seen in nascent primitive streak and emerging mesoderm. *Mixl1* expression was maintained in emerging mesoderm in mid- to late-streak embryos, becoming restricted to the posterior primitive streak by the head-fold stage. Expression was not seen in the node or in endoderm flanking the node. In early somite stage embryos, expression was detectable in the crown cells of the caudal notochord and in primitive streak (Pearce and Evans, 1999; Robb et al., 2000). A single human *Mixl1* homolog has been identified (Robb et al., 2000).

To establish the role of *Mixl1* in murine development, we created a mouse strain bearing a targeted mutation of the *Mixl1* gene. Gastrulation stage *Mixl1*-null embryos had abnormalities in primitive streak and node formation. Post-gastrulation, *Mixl1* mutants exhibited complex defects in axial mesodermal and endodermal structures, suggesting a role for *Mixl1* in the regulation of morphogenetic cell movements associated with gastrulation. Despite the defects in early morphology and terminal differentiation of trunk organizer cells, gene marker studies indicated that their inductive properties were maintained. Moreover, in chimera studies, *Mixl1*-null embryonic stem cells were found to contribute poorly to gut endoderm, thereby implicating *Mixl1* in endoderm patterning.

MATERIALS AND METHODS

Generation of *Mixl1* mutant mice

A 5′ 4 kb fragment of the *Mixl1* genomic locus which included the *Mixl1* translational start was cloned in frame with EGFP in the vector pEGFPKT1LOXNEO (Godwin et al., 1998). A 1.9 kb fragment of the *Mixl1* genomic locus incorporating intron 1 and exon 2 was inserted at the 3′ end of the loxP-flanked neomycin selection cassette to complete the *Mixl1* targeting vector. The W9.5 embryonic stem (ES) cell line was maintained, electroporated and selected with G418 as described (Robb et al., 1995). Homologous recombinants were identified by Southern analysis of *Hin*dIII-digested DNA isolated from individual clones. Southern blots were hybridized with the 3′ genomic DNA probe (Fig. 1A). The targeted deletion was confirmed by further analysis of Southern analysis of DNA from selected clones with the 5′ genomic DNA probe (Fig. 1A). Two targeted clones were injected into C57BL/6 blastocysts and chimeric offspring were bred to 129Sv or C57BL/6 mice to derive mice heterozygous for the *Mixl1* mutation ($Mixl1^{+/-}$) or to *Cre* transgenic mice (Schwenk et al., 1995) to create mice heterozygous for a targeted *Mixl1* allele lacking the neomycin selection cassette ($Mixl1^{+/\Delta neo}$).

Genotyping

Adult heterozygote $Mixl1^{+/-}$ and $Mixl1^{+/\Delta neo}$ mice were genotyped by Southern analysis of *Hin*dIII-digested tail DNA using the 3′ probe. Adult mice and embryos were also identified by PCR analysis using tail and embryonic yolk sac DNA (Moens et al., 1993). Tissue was digested in a buffered non-ionic detergent solution (100 ng/ml proteinase K, 50 mM KCl, 10 mM Tris.HCl (pH 8.3), 2.0 mM $MgS0_4$, 0.45% Nonidet P-40, 0.45% Tween-20) for 3 hours to overnight followed by inactivation of proteinase K activity at 100°C for 10 minutes. Samples (1 μl) were analyzed in a 10 μl *Taq* DNA polymerase PCR reaction, as described by the manufacturer (Invitrogen). To amplify the wild-type and $Mixl1^{-}$ alleles, a mixture of three primers was used in the same reaction: In1a, 5′-CTTCCTGCTGGGACCTTTCAATGG-3′; Ex1a, 5′-TCGTCTT-CCGACAGACCATGTACC-3′; and Neo1a, 5′-CTGACCGCTTCC-TCGTGCTTTACG-3′. To amplify the wild-type and $Mixl1^{\Delta neo}$ alleles, the primer GFP1a (5′-ATGGACGAGCTGTACAA-GTAAAGCG-3′) replaced primer Neo1a. Embryos between 6.75 and 8.5 dpc were also genotyped by analysis of EGFP fluorescence using a Leica MZFLIII dissecting microscope using a mercury lamp and GFP2 filter system.

Fluorescence imaging

Embryos obtained from timed matings of $Mixl1^{+/-}$ or $Mixl1^{+/\Delta neo}$ pairs were harvested and maintained at room temperature in Hepes-buffered Eagles Medium without Phenol Red during imaging with a Leica TCS-SP2 Confocal Imaging System connected to a Leitz Arisoplan microscope. Thick sections for confocal imaging were cut using disposable steel blades (Probing and Structure).

In situ hybridization and histology

For histology, embryos were fixed in 4% paraformaldehyde, dehydrated through an ethanol series and embedded in paraffin wax. Blocks were sectioned at 6 μm, dewaxed and stained in Hematoxylin and Eosin. Embryos for whole-mount in situ hybridization were fixed in 4% paraformaldehyde and stored at 4°C. Hybridization was performed as described (Belo et al., 1997). After hybridization, stained embryos were refixed in 4% paraformaldehyde. Selected embryos were dehydrated, embedded in paraffin wax and sectioned at 10 μm.

Mixl1-null ES cell derivation and generation of chimeric embryos

Wild-type R26.1 ES cells, which are derived from a mouse carrying the ROSA-26 *lacZ* gene trap (Varlet et al., 1997), were injected into blastocysts obtained by mating $Mixl1^{+/-}$ and $Mixl1^{+/\Delta neo}$ animals. Chimeras derived from $Mixl1^{-/\Delta neo}$ blastocysts were identified by PCR of yolk sac DNA, using the primers pairs described above. PCR of $Mixl1^{-/\Delta neo}$ yolk sac DNA gave rise to products specific for the $Mixl1^{-}$ allele and the $Mixl1^{\Delta neo}$ allele, in addition to the wild-type (maternally

derived) allele. *Mixl1*$^{-/\Delta neo}$ ES cell lines were generated by first using CRE-mediated recombination to remove the loxP-flanked neomycin resistance cassette from a *Mixl1*$^{+/-}$ ES cell line, thereby creating *Mixl1*$^{+/\Delta neo}$ cell lines. The second allele was then replaced by a further round of gene targeting with the original targeting construct. Two *Mixl1*$^{-/-}$ ES cell lines were identified by Southern analysis of *Hin*dIII-digested DNA using the 3′ probe to detect the 4.7 kb and 3.7 kb mutant alleles. The correct targeting of the locus was confirmed by further Southern analysis. Chimeric embryos were generated by injection of *Mixl1*$^{-/-}$ ES cells into blastocysts carrying the ROSA-26 *lacZ* transgene. β-Galactosidase activity in chimeric embryos was detected by X-gal histochemistry (Elefanty et al., 1999). Stained embryos were post-fixed and sectioned at 10 μm.

Nodal expression analysis

Nodal$^{+/lacZ}$ mice, generously provided by Liz Robertson, were bred with *Mixl1*$^{+/-}$ mice. The offspring were genotyped for *Mixl1* as above and for *Nodal* as described (Collignon et al., 1996). Compound heterozygotes were interbred and offspring genotyped by PCR of yolk sac DNA. β-galactosidase activity was detected as described elsewhere (Elefanty et al., 1999).

RESULTS

Mixl1 mutants display abnormalities of the primitive streak and midline structures

To investigate the role of *Mixl1* in mammalian development, a loss-of-function mutation was generated. The *Mixl1*-coding sequence in exon 1 was replaced, in frame, by a cassette encoding the enhanced green fluorescent protein (GFP) and neomycin resistance (Fig. 1A). An ES cell line that had undergone homologous recombination was used to generate chimeric mice. Chimeras were bred to 129Sv or C57BL/6 mice to derive offspring heterozygous for the *Mixl1* mutation (*Mixl1*$^{+/-}$) or to *Cre* transgenic mice (Schwenk et al., 1995) to create offspring heterozygous for a targeted *Mixl1* allele lacking the neomycin selection cassette (*Mixl1*$^{+/\Delta neo}$) (Fig. 1B). Both *Mixl1*$^{+/-}$ and *Mixl1*$^{+/\Delta neo}$ mice appeared normal and were fertile. Heterozygous intercrosses never yielded viable homozygous offspring, indicating embryonic lethality. In litters produced by mating *Mixl1*$^{+/-}$ or *Mixl1*$^{+/\Delta neo}$ mice, homozygous *Mixl1* mutant embryos were present in the expected Mendelian ratio at 7.5 dpc, but were absent after 10.5 dpc. The phenotype of homozygous embryos (hereafter referred to as *Mixl1*$^{-/-}$ or mutant embryos) that were derived from matings of either *Mixl1*$^{+/-}$ or *Mixl1*$^{+/\Delta neo}$ heterozygous mice was indistinguishable and results from the analyses were therefore pooled. Examination of *Mixl1* expression in wild-type and *Mixl1*$^{-/-}$ 7.5 dpc embryos by whole-mount in situ hybridization showed a complete lack of *Mixl1* transcripts (data not shown).

After homologous recombination, the *GFP* reporter and the neomycin selection cassette replaced most of *Mixl1* exon 1, leaving potential 5′, 3′ or intronic regulatory sequences intact. In keeping with pattern of *Mixl1* RNA expression, the visceral endoderm, primitive streak and nascent mesoderm of gastrulation stage *Mixl1*$^{+/-}$ embryos expressed GFP. Fluorescence was first detected at 6.5 dpc, 1 day after *Mixl1* RNA was detectable by whole-mount in situ hybridization (Pearce and Evans, 1999; Robb et al., 2000) and GFP signal in *Mixl1*$^{+/-}$ embryos persisted in visceral endoderm up to the late bud stage. Co-incident with the *Mixl1* mRNA expression at 7.5 dpc, maximal fluorescence was seen in the primitive streak and mesodermal wings at this time (Fig. 1C,F). At 8.25 dpc, fluorescence was confined to the posterior primitive streak of *Mixl1*$^{+/-}$ embryos, and by 9.0 dpc was completely absent, mirroring the *Mixl1* mRNA expression pattern (data not shown). In *Mixl1*$^{-/-}$ embryos, the fluorescence was brighter than in *Mixl1*$^{+/-}$ embryos and remained detectable until 9.5 dpc (Fig. 1D,F and not shown).

At 6.5 dpc, *Mixl1*$^{-/-}$ embryos are morphologically indistinguishable from their littermates. However by 7 dpc, at the mid-streak stage, *Mixl1*$^{-/-}$ embryos display a thickened primitive streak and lack a morphologically recognizable node at the anterior end of the primitive streak (Fig. 2A,F). An excess of mesoderm-like cells accumulates in the anterior streak and in the region immediately lateral to the primitive streak (Fig. 2B-E,G-J). The early-neural plate stage (7.75 dpc) *Mixl1*$^{-/-}$ embryos are retarded in the elevation of neural folds and develop a shallow anterior intestinal portal (data not shown). At the early somite-stage (8.5 dpc), the embryos adopt a flattened disc morphology instead of a lordotic shape and the anteroposterior (AP) axis is markedly foreshortened (Fig. 3A-C). The neural folds are small and disorganized and very little head mesenchyme is found underneath the head folds (Fig. 3I-M). The heart tube is absent (Fig. 3I,J). The foregut invagination is rudimentary and no hindgut portal is formed (Fig. 3I,L,M). From two to five pairs of somites are formed in the paraxial mesoderm flanking a thick axial mass of flattened neurectoderm overlying a condensed core of mesodermal tissues that replaced the notochord.

Rarely, *Mixl1*$^{-/-}$ embryos with severely disorganized head folds were recovered from 9-9.5 dpc litters. These embryos failed to turn and did not form a heart tube (Fig. 3D, Fig. 4A-E). In the 20 9.5 dpc *Mixl1*$^{-/-}$ embryos examined, the axial tissue mass present at 8.5 dpc had grown in size, and developed into a huge mass of tail bud-like tissue protruding dorsally from the caudal region of the embryo (Fig. 3D, Fig. 4A,B,E). In some embryos, an additional bulbous tissue forms ectopically in the trunk of the embryo (Fig. 4B,D), giving an impression that the embryonic axis is bifurcated. Analysis of *Brachyury* expression shows that axial tissues in these mutants are discontinuous along the body axis. *Brachyury* is expressed in a poorly organized structure that resembles the notochordal plate and in a notochord-like structure that ends caudally, either in an ectopic protrusion (arrows in Fig. 4B,D) or in a bulbous mass (Fig. 4E).

In the mutants, the fusion of the posterior and anterior amniotic folds is delayed, leading to persistence of the proamniotic canal as late as the late bud/early head fold stage (Fig. 2F). The differentiation of extra-embryonic tissue in 8.5 dpc *Mixl1*$^{-/-}$ conceptuses appears normal. Blood islands are plentiful in the yolk sac of *Mixl1*$^{-/-}$ embryos (Fig. 3J). However, in comparison with wild-type littermates, the allantois of *Mixl1*$^{-/-}$ embryos appeared disproportionately large in size (Fig. 3B).

Loss of *Mixl1* function results in enhanced *Brachyury* and *Nodal* expression

Brachyury (*T*), which is expressed in the primitive streak and axial mesoderm of the wild-type 7.5 dpc embryo (Wilkinson et al., 1990), is expressed in an expanded domain in both the epiblast and mesenchymal components of the thickened

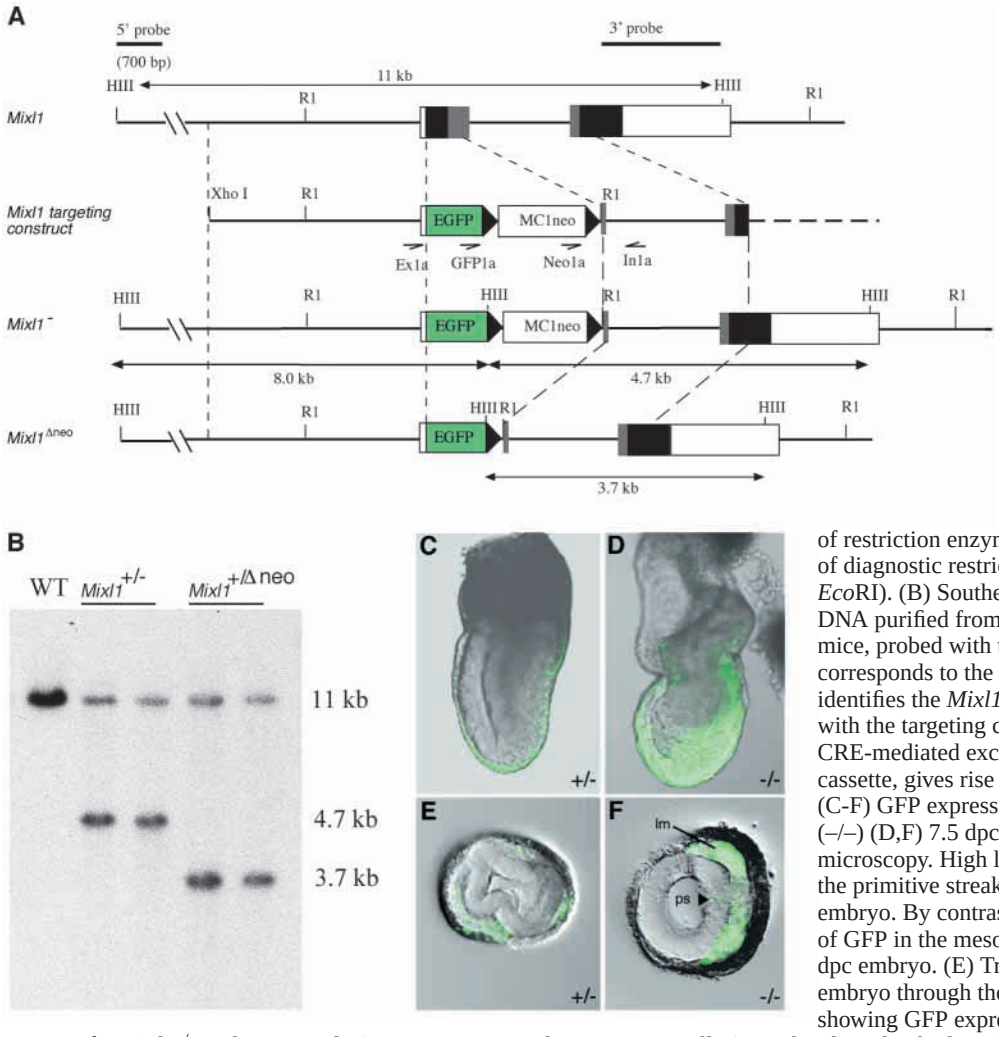

Fig. 1. Targeted mutation of *Mixl*. (A) Genomic organization of the *Mixl1* locus and structure of the targeting vector. Boxes indicate exons, coding sequence is filled, with the homeodomain indicated by lighter shading. A mutant allele (*Mixl1*$^{-}$) is produced by replacing exon 1 downstream of the ATG with an EGFP loxP-MC1-neo-loxP cassette. Excision of the floxed MC1neo sequence by Cre-recombinase generates the allele *Mixl1*$^{\Delta neo}$. Positions of 5′ and 3′ genomic DNA probes and PCR primers are indicated. The positions of restriction enzymes are shown, together with the sizes of diagnostic restriction fragments (HIII, *Hin*dIII; RI, *Eco*RI). (B) Southern blot analysis of *Hin*dIII-digested DNA purified from wild-type, *Mixl1*$^{+/-}$ and *Mixl1*$^{+/\Delta neo}$ mice, probed with the 3′ probe. The 11 kb band corresponds to the wild-type *Mixl1* allele. The 4.7 kb band identifies the *Mixl1* allele after homologous recombination with the targeting construct. The targeted allele, after CRE-mediated excision of the neomycin resistance cassette, gives rise to a 3.7 kb band. WT, wild type. (C-F) GFP expression in *Mixl1*$^{+/-}$ (+/–) (C,E) and *Mixl1*$^{-/-}$ (–/–) (D,F) 7.5 dpc embryos visualized by confocal microscopy. High levels of GFP expression are found in the primitive streak and lateral mesoderm of the *Mixl1*$^{-/-}$ embryo. By contrast, a lower and more uniform expression of GFP in the mesoderm is observed in the *Mixl1*$^{+/-}$ 7.5 dpc embryo. (E) Transverse section of a *Mixl1*$^{+/-}$ 7.5 dpc embryo through the middle level of the primitive streak, showing GFP expression in the mesoderm. (F) Transverse section of a *Mixl1*$^{-/-}$ embryo reveals GFP expression in the ingressing cells (arrowhead) in the thickened primitive streak (ps) and the nascent mesoderm (lm) located lateral to the primitive streak.

primitive streak and in the adjacent mesodermal cells in the *Mixl1*$^{-/-}$ embryos (Fig. 5A-D). In 8.25 dpc mutant embryos, *Brachyury* is expressed in an irregular and broad strip of mesodermal cells underlying the midline of the head fold and neural plate along the AP axis. (Fig. 5E-G). Histological examination reveals that *Brachury* is expressed in ventral tissues of the open neural plate that resemble the floor plate of the neural tube (Fig. 5H). In the posterior region of the mutant embryo, *Brachyury* is expressed in the superficial layer of cells of the primitive streak and in the ventral-most tissues that appear to have organized into a notochordal plate-like structure (Fig. 5I). In contrast to the uniform expression in the primitive streak of wild-type embryo, expression is excluded from the core of the primitive streak (Fig. 5I).

We also examined the expression of *Nodal* in *Mixl1*$^{-/-}$ embryos. Expression of *Nodal* was assessed in *Mixl1* mutant embryos that are heterozygous for *Nodal*^{lacZ}, a null allele generated by integration of a *lacZ* transgene into the *Nodal* locus that provides a reporter for *Nodal* expression (Collignon et al., 1996). *Nodal* expression in the wild-type embryo is very dynamic, being initially expressed throughout the epiblast at 6.5 dpc, then localizing to the primitive streak before being restricted to a horseshoe-shaped domain around the node by 8 dpc (Zhou et al., 1993; Conlon et al., 1994; Varlet et al., 1997). In the mid- to late-streak stage, *Mixl1*$^{-/-}$ mutant embryo, the domain of *Nodal* expression in the epiblast and the primitive streak is significantly expanded (Fig. 5J). In older mutants, *Nodal* expression spreads more widely in the posterior midline, but is absent from lateral plate mesoderm (Fig. 5K,L).

Tissues in the midline display the molecular properties of axial mesendoderm

In the wild-type embryo, *Foxa2* (*HNF3β*) expression is localized to the anterior primitive streak, the node and the anterior mesendoderm at 7.5 dpc and at early somite stages marks axial midline structures such as notochord, floor plate and gut endoderm (Ang et al., 1993; Monaghan et al., 1993; Ruiz i Altaba et al., 1993; Sasaki and Hogan, 1993). In 7.5 dpc *Mixl1*$^{-/-}$ embryos, an expanded domain of expression of *Foxa2* is found in the mesendodermal tissues in distal region of the gastrula-stage embryo at the anterior end of the primitive streak (Fig. 6A,B). At 8.25 dpc, *Foxa2* is present in the axial tissues over most of the length of the embryonic axis of the mutant embryos (Fig. 6C,F). Sonic hedgehog (*Shh*) is

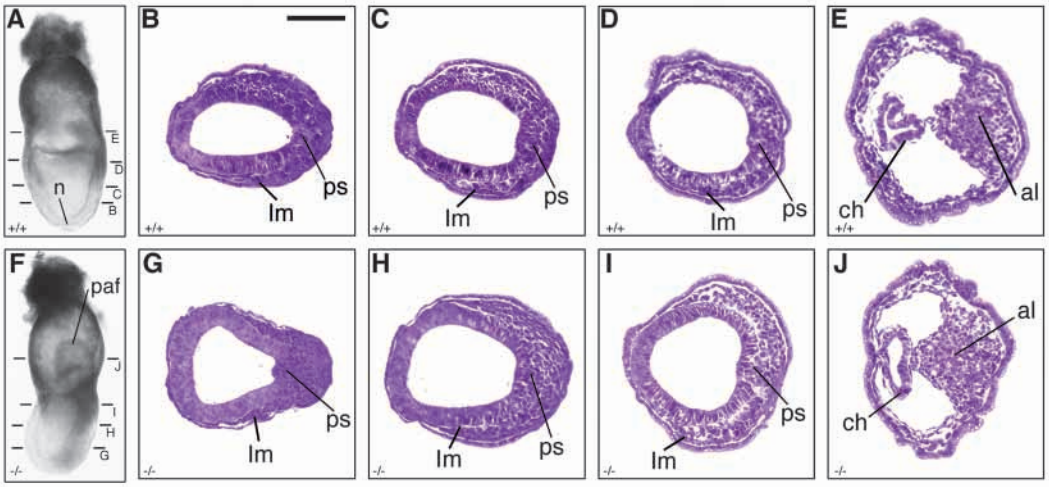

Fig. 2. *Mixl1*$^{-/-}$ embryos show an accumulation of mesenchymal cells in the thickened primitive streak and adjacent mesoderm. Lateral views of an early-bud stage wild-type (+/+) embryo (A) and a mid-streak stage *Mixl1*$^{-/-}$ (–/–) (F) embryo. The *Mixl1*$^{-/-}$ embryo has a thickened primitive streak, lacks a node (n) and shows delay in closure of the amnion (paf, posterior amniotic fold). Transverse sections through wild-type (B-E) and *Mixl1*$^{-/-}$ (G-J) embryos at the levels indicated in A,F, showing the congregation of cells in the anterior segment of the primitive streak (ps) and adjacent mesoderm (lm) in the mutants. The allantois (al) and chorion (ch) are morphologically similar in the wild type and mutant. Scale bar: 25 μm.

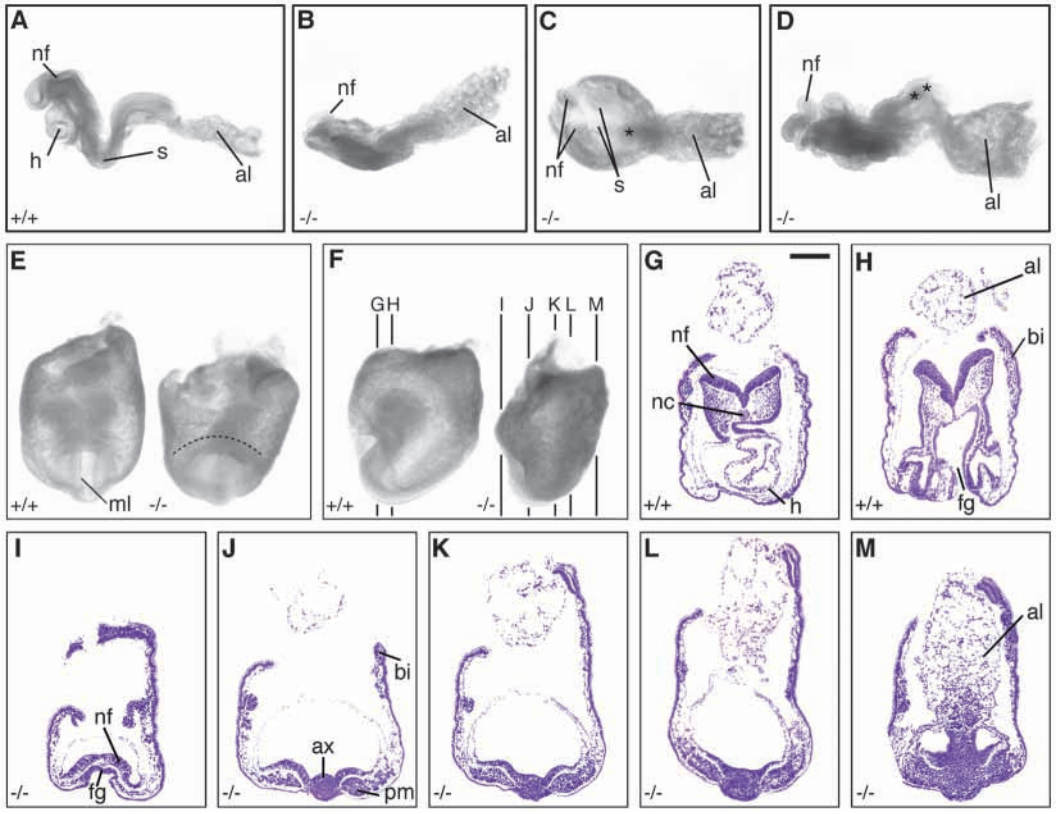

Fig. 3. Early somite stage *Mixl1*$^{-/-}$ embryos exhibit multiple developmental abnormalities. (A-C) Lateral view of a five-somite wild-type (+/+) embryo (A), and lateral (B) and dorsal (C) views of a three-somite *Mixl1*$^{-/-}$ (–/–) littermate. The *Mixl1*$^{-/-}$ embryos do not adopt the lordotic morphology of the wild-type embryo, develop no heart and form a large allantois. The asterisk indicates the midline tissue mass separating the somites (s). (D) A 9.0 dpc *Mixl1*$^{-/-}$ embryo showing disorganization of the neural folds and the formation of a bulbous caudal protrusion (double asterisks). (E,F) Anterior (E) and lateral (F) views of 8.25 dpc wild-type and *Mixl1*$^{-/-}$ conceptuses. Note the absence of clearly defined midline structures (ml) in the *Mixl1*$^{-/-}$ embryo. The silhouette of collapsed head folds of the mutant is outlined by a broken line. (G-M) Histological sections of 8.25 dpc wild-type and *Mixl1*$^{-/-}$ conceptuses, at planes indicated in F. Note the poorly developed neural folds and foregut portal in the mutant. A compact core of cells (ax, J) is found in the midline in place of the notochord. Abbreviations: allantois (al), blood islands (bi), foregut portal (fg), heart (h), notochord (nc), neural folds (nf) and paraxial mesoderm (pm). Scale bar for histological sections: 50 μm.

first detected at the late streak stage in the anterior mesendoderm, which extends rostrally from the primitive streak, and during organogenesis, in the node, head process, notochord, prechordal plate, floorplate and endoderm in the dorsolateral region of the embryonic gut (Echelard et al., 1993; Roelink et al., 1994). In the late-streak stage *Mixl1*$^{-/-}$embryos, *Shh* expression is restricted to cells clustered near the anterior end of the streak (Fig. 6G,H). In 8.25 dpc mutants, weak, poorly localized *Shh* expression is seen in the ventral part of the condensed axial tissue that resembles the notochordal plate (Fig. 6I-L). *Gsc*, which marks the prechordal plate in late head-fold-stage embryos, is expressed in the mesendoderm in the anterior region of the mutants (data not shown). Overall, the marker studies showed

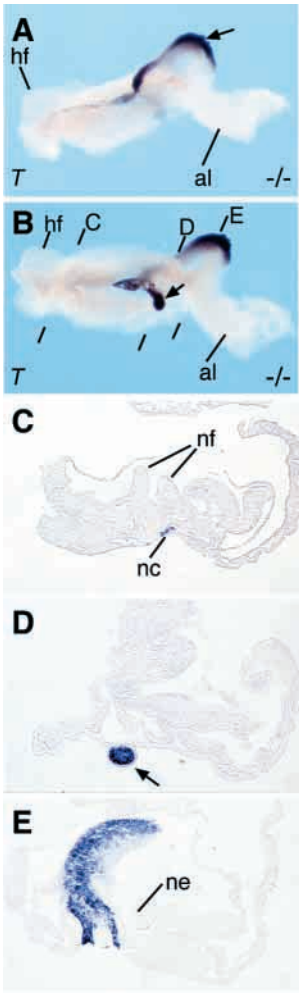

Fig. 4. Excessive growth of axial mesoderm and bifurcation of the embryonic axis in 9-9.5 dpc *Mixl1*$^{-/-}$ embryos. (A) Dorsolateral view of a mutant embryo showing *Brachyury* (*T*)-expressing tissues in the bulge (arrow) formed at the caudal end of the embryonic axis and (B) ventral view of the same embryo showing the protrusion derived from the axial tissue mass (arrow). (C-E) Histological sections at the planes indicated in B show (C) *T* expression in the flat notochord-like structure, (D) the protruding tissues on the ventral side of the embryo (arrow indicates the same structure shown in B) and (E) the bulge that extends dorsally through a split in the neural plate. hf, head fold; al, allantois; nc, notochord-like structure; ne, neuroectoderm; nf, neural fold.

that tissues displaying the molecular characteristics of axial mesendoderm are specified in the *Mixl1*$^{-/-}$ embryos, despite proper axial structures not being formed.

Paraxial mesoderm, presumptive cardiogenic mesoderm and anterior neural primordium express proper molecular characteristics

In the *Mixl1*$^{-/-}$ embryos, *Twist* is expressed in the presumptive paraxial mesoderm in the posterior region of the embryo and the allantoic mesoderm. However, unlike wild-type embryos, *Twist* expression is not seen in the mesoderm underneath the presumptive cranial neural plate or in lateral plate mesoderm (Fig. 6M,N). *Meox1*, which marks the paraxial presomitic mesoderm and segmented somites of wild-type embryos, is also expressed in the paraxial mesoderm of the 8.5 dpc mutant embryos (data not shown). In early somite stage wild-type embryos, *Cer1* is expressed in the anterior presomitic mesoderm and in two to three newly formed somites (see Fig. 8A). *Cer1* expression is maintained in the paraxial mesoderm and the somites of the mutant embryo (see Fig. 8B,C). The absence of the heart tube in *Mixl1*$^{-/-}$ embryos may reflect a defect in cardiomyocyte specification or a morphogenetic defect in heart tube formation. In wild-type embryos, *Nkx2.5* is expressed strongly in the cardiogenic mesoderm and later in the myocardium (Lyons et al., 1995). In 8.0 dpc *Mixl1*$^{-/-}$ embryos, *Nkx2.5* is expressed ectopically in the mesoderm present bilaterally in the anterior region of the embryo. This finding suggests that cardiogenic mesoderm is specified in the absence of *Mixl1* but the progenitors fail to undergo heart tube morphogenesis (Fig. 6O,P). Despite the abnormal development of the anterior region of the *Mixl1*$^{-/-}$ embryos, expression of the prospective forebrain and the anterior neural ridge marker *Six3* (Oliver et al., 1995) and *Otx2* (Ang et al., 1993; Simeone et al., 1993) is correctly localized to the abnormal neural tube of the mutant embryos (Fig. 6Q,R and data not shown).

Definitive endoderm is specified but gut morphogenesis is defective in *Mixl1* mutants

During embryogenesis, definitive endoderm cells originate from the primitive streak and intercalate into the visceral endoderm layer, displacing these cells to the vitelline yolk sac (Lawson and Pedersen, 1987). We examined this morphogenetic process in *Mixl1*$^{-/-}$ embryos by assessing the expression of *Pem* (Lin et al., 1994) and α-fetoprotein (*Afp*) (Dziadek and Adamson, 1978), which mark the formation of the visceral endoderm. At 7.5 dpc, expression of *Pem* (not shown) and *Afp* in *Mixl1*$^{-/-}$ embryos was similar to that in wild-type embryos, indicating the visceral endoderm has been displaced to the extra-embryonic region by the definitive endoderm in the mutant embryo (Fig. 7A-D).

The expression of *Cer1* and *Sox17* were examined to assess differentiation and patterning of the endoderm. *Cer1* and *Sox17* are first expressed in the anterior visceral endoderm of early streak stage embryos and in anterior definitive endoderm in the late-streak stage embryo. At the head fold stage, both genes are expressed in the definitive endoderm of the prospective foregut pocket. By the early somite stage *Cer1* expression in endoderm wanes and *Sox17* expression becomes confined to hindgut (Belo et al., 1997; Biben et al., 1998; Shawlot et al., 1998; Kinder et al., 2001; Kanai-Azuma et al., 2002). At 7.5 dpc *Cer1* and *Sox17* are expressed in the anterior endoderm of *Mixl1*$^{-/-}$ embryos, in a pattern comparable with that of wild-type littermates (Fig. 7E-H). However, there is an evident reduction in the population of *Sox17*-expressing cells in the prospective foregut endoderm (Fig. 7G,H). By 8.5 dpc, *Cer1* expression is no longer detected in the anterior endoderm of wild-type littermates but is retained in endoderm in the region of the presumptive foregut invagination of the *Mixl1*$^{-/-}$ embryos (Fig. 8A-D). *Sox17*, which is expressed in the mid- and hindgut of the wild-type embryo, is ectopically expressed in the endoderm in the rudimentary structure that is reminiscent of the foregut portal (Fig. 8E-H). Taken together, these results indicate that definitive endoderm has been specified in *Mixl1*$^{-/-}$ embryos. However, the lethality of the mutant embryos precludes further analysis of the morphogenesis and differentiation of the endodermal derivatives.

Mixl1 activity in epiblast is required for normal axial patterning and the expression of endodermal potency

As *Mixl1* is expressed in both the epiblast and extra-embryonic tissues during gastrulation (Pearce and Evans, 1999; Robb et al., 2000), it is possible that the proper inductive interactions do not exist between these tissues in the *Mixl1*$^{-/-}$ embryos. In order to identify the tissues in which *Mixl1* is required for axial mesoderm patterning, we generated mouse chimeras containing

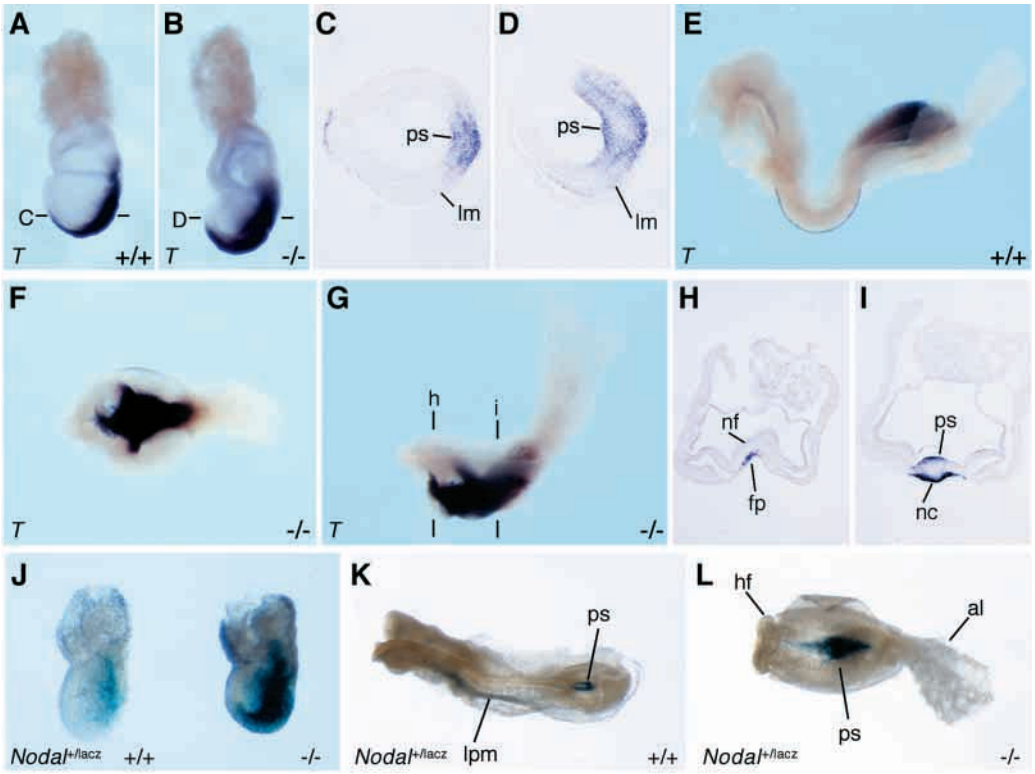

Fig. 5. *Brachyury* (*T*) and *Nodal* expression domains are expanded in *Mixl1*$^{-/-}$ embryos. (A-D) *T* is expressed in a wider domain in 7.5 dpc late-bud stage *Mixl1*$^{-/-}$ (–/–) mutant embryos (B) than in the wild-type (+/+) embryo (A). Transverse sections (C,D), at the levels shown in A,B reveal that *T* expression in the mutant embryo is extended more laterally from the primitive streak (ps) to encompass the adjacent lateral mesodermal (lm) cells. (E) Lateral view of an early somite stage wild-type embryo, and dorsal (F) and lateral (G) views of the mutant embryo showing the expanded *T* expression domain in the mutant embryo, which may be accentuated by the foreshortening of the anterior part of the embryo. (H,I) Histological sections of the mutant embryo at planes shown in G, showing the *T*-expressing cells in the notochord-like structure (nc) under the neural folds (nf), and in the dorsal superficial cells in the primitive streak (ps) and the ventral mesendodermal tissue sheet that resembles the notochordal plate (ncp). (J) *Nodal* ^{lacZ} expression is expanded in the posterior tissues of the late-streak stage *Mixl1*$^{-/-}$ embryos. In the wild-type 8.5 dpc embryo (K), *Nodal* ^{lacZ} is expressed in the perinodal tissues of the primitive streak (ps) and the left lateral plate mesoderm (lpm). In the mutant embryo (L), which displays small head folds (hf) and an enlarged allantois (al), *Nodal*^{lacZ} is expressed strongly in an expanded domain in the anterior segment of the primitive streak (ps) and in the axial tissues immediately anterior to the primitive streak.

wild-type epiblast cells and *Mixl1*-deficient visceral endoderm and trophectodermal derivatives. Descendants of the wild-type R26.1 ES cells in the epiblast can be identified by the constitutive expression of a ROSA-26 *lacZ* transgene (Friedrich and Soriano, 1991; Varlet et al., 1997). These ES cells were injected into *Mixl1*$^{-/\Delta neo}$ blastocysts obtained by mating *Mixl1*$^{+/-}$ and *Mixl1*$^{+/\Delta neo}$ mice. (This mating strategy was employed to facilitate genotyping of the chimeras – see Materials and Methods.) In the chimeras, wild-type ES cells contribute efficiently to embryonic, but rarely to extra-embryonic, lineages (Beddington and Robertson, 1989; Varlet et al., 1997). If *Mixl1* expression in visceral endoderm is essential, wild-type ES cells will not rescue the defects of *Mixl1*$^{-/-}$ host blastocysts. Five 8.5 dpc *Mixl1*$^{-/-}$ blastocyst-derived chimeras that contained a greater than 50% contribution from wild-type (*lacZ*-positive) ES cells were phenotypically indistinguishable from chimeric embryos derived from wild-type or *Mixl1*$^{+/-}$ host blastocysts and wild-type ES cells. The rescue of the mutant phenotype by the presence of wild-type cells in the embryo containing *Mixl1*-deficient extra-embryonic ectoderm and visceral endoderm indicates that loss of *Mixl1* function in the extra-embryonic tissues is unlikely to have caused the disruption in embryogenesis.

The requirement for *Mixl1* in embryonic development was studied in a reciprocal experiment. Two independent *Mixl1*$^{-/\Delta neo}$ ES cell lines were derived by a second round of targeted mutation of the normal *Mixl1* allele of a *Mixl1*$^{+/\Delta neo}$ ES cell line using the original targeting construct (see Materials and Methods). Chimeras were produced by introducing *Mixl1*$^{-/\Delta neo}$ ES cells (identified by the lack of *lacZ* expression) into *Mixl1*$^{+/+}$ ROSA-26 transgenic blastocysts. A proportion of the chimeric embryos with a high contribution of *Mixl1*$^{+/\Delta neo}$ ES cells phenocopied the defective development of the *Mixl1*$^{-/-}$ mutants, demonstrating that normal *Mixl1* activity in visceral endoderm is not sufficient to compensate for the deficiency in the embryonic tissues (Fig. 9A). Chimeras with 20% or more wild-type cells showed partial to nearly complete rescue of developmental defects. Histological examination of these chimeras reveals that *Mixl1*$^{-/-}$ cells can colonize most embryonic tissues, including the neural tube and the notochord. However *Mixl1*$^{-/-}$ cells consistently display low level of contribution to the heart and foregut and are almost completely excluded from the endoderm of the midgut and hindgut (Fig. 9B-F)

DISCUSSION

Mixl1 function is crucial for the morphogenesis of germ layer derivatives

During mouse development, absence of *Mixl1* activity results in abnormal germ layer morphogenesis during gastrulation, the absence of a morphologically distinct node and formation of a condensed core of mesodermal tissues in place of the notochord. The *Mixl1*$^{-/-}$ embryos do not form a heart, fail to

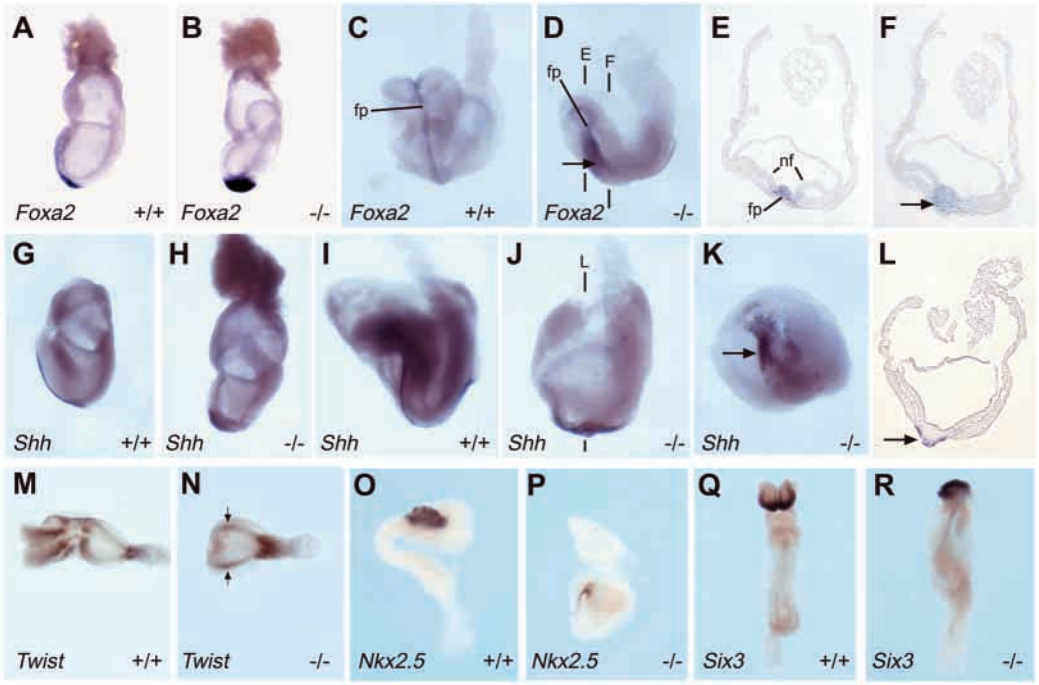

Fig. 6. Expression of markers of axial mesendoderm, paraxial mesoderm and cardiac mesoderm is maintained in *Mixl1*$^{-/-}$ embryos. (A,B) Lateral views of wild-type (+/+) (A) and *Mixl1*$^{-/-}$ (–/–) (B) 7.5 dpc embryos showing the expanded *Foxa2* expression domain in the tissues anterior to the primitive streak. (C-F) Frontal views of early somite stage wild-type (+/+) and *Mixl1*$^{-/-}$ (D) embryos, and histological sections (E,F) taken at the planes indicated in D. *Foxa2* is expressed in the floor plate (fp) and notochord of the wild-type embryo and in the compact tissue mass in the midline of the mutant embryo (arrows in D,F). (G,H) Lateral views of wild-type (G) and *Mixl1*$^{-/-}$ (H) 7.5 dpc embryos showing that *Shh* is expressed in a cell cluster near the anterior end of the streak in the mutant embryo, but expression is not extended to the more anterior axial tissues as in the wild-type embryo. At 8.5 dpc (I-L), *Shh* is expressed only in the ventral part (arrow in L) of the midline axial mass of the mutant embryo. (I,J) Lateral views, (K) anteroventral view, (L) histological section (plane indicated in J). (M,N) *Twist* expression is maintained in *Mixl1*$^{-/-}$ embryos (N) in the mesoderm at the base of the allantoic bud and the presumptive lateral plate mesoderm, similar to that in the early somite stage wild-type embryos (M). However, unlike wild-type embryos, *Twist* expression is absent from the mesoderm underneath the rudimentary cranial neural plate. (N) Dorsal view showing *Twist* expression in the lateral mesoderm (arrows). (O,P) Expression of the *Nkx2.5* in the heart tube of wild-type embryos (O, lateral view) and in a poorly defined crescent-shaped patch of cells in *Mixl1*$^{-/-}$ embryos (P, anterior view), but no heart is formed. (Q,R) Ventral views of early-somite stage wild-type and *Mixl1*$^{-/-}$ embryos showing *Six3* expression in the prospective ventral forebrain.

elongate along the AP axis, develop a vestigial foregut and are mostly arrested in development by 9 dpc. Analysis of the expression of molecular markers for germ layer derivatives in the mutant embryos reveals that the progenitors of the neural, mesodermal and endodermal lineages are all present and the precursor tissues are properly patterned during gastrulation and early neurulation. In a few *Mixl1*$^{-/-}$ embryos that developed to 9.5 dpc, a poorly organized notochord-like structure was formed in the midline of the grossly malformed neural tube and a mass of *T*-expressing tissues that resembles an overgrown tail bud was found at the caudal end of the axis. In some embryos, an outgrowth of *T*-expressing tissues protruded from the ventral side of the trunk as if the embryonic axis had bifurcated. The phenotypic consequences of *Mixl1* mutation strongly suggest that *Mixl1* function is crucial for the morphogenesis of germ layer derivatives and axis development.

Mixl1 function is essential for endoderm differentiation

The defective morphogenesis of the embryonic gut in the

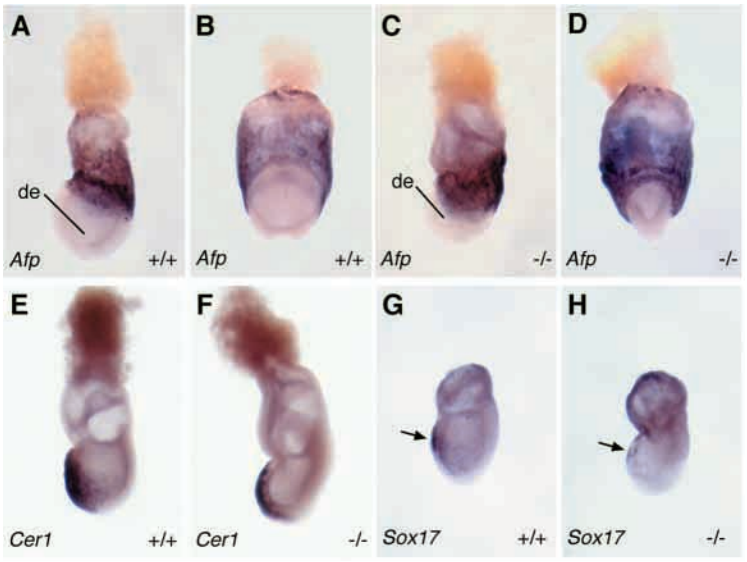

Fig. 7. Endoderm is specified in *Mixl1*$^{-/-}$ embryos. (A-D) Expression of *Afp* in 7.5 dpc wild-type (+/+) (A,B) and *Mixl1*$^{-/-}$ (–/–) embryos (C,D). Lateral (A,C) and anterior views (B,D) showing *Afp* expression in the visceral endoderm of the vitelline yolk sac, but not in the definitive endoderm (de). The *Afp* expression domain seems to extend more distally in the mutant embryo. (E,F) *Cer1* is expressed in anterior definitive endoderm of the late bud/early head fold stage *Mixl1*$^{-/-}$ embryo (F) and of the early bud stage wild-type embryo (E). (G,H) *Sox17* is expressed in the anterior definitive endoderm of the early-bud wild type and *Mixl1*$^{-/-}$ embryo (arrows).

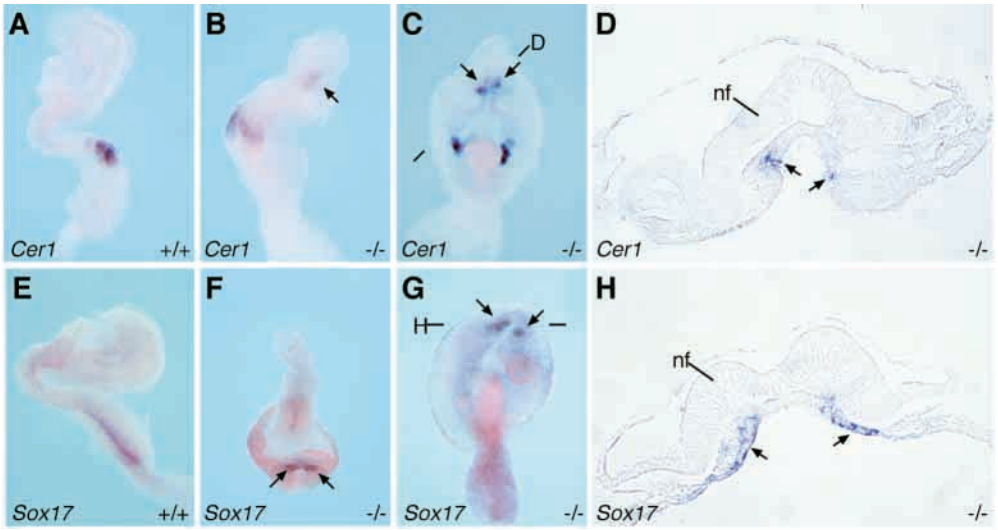

Fig. 8. Expression of *Cer1* and *Sox17* in the presumptive foregut of *Mixl1*$^{-/-}$ embryos. (A-C) Lateral (A,B) and dorsal (C) views of *Cer1* expression in wild-type (+/+) (A) and *Mixl1*$^{-/-}$ (–/–) embryos (B,C, same specimen). Expression is seen in the two newly formed somites and anterior presomitic mesoderm in both wild-type and mutant embryos, but ectopic expression (arrows) is found in the endoderm of the presumptive foregut of the mutant embryo. (D) Histological section at the plane shown in C shows *Cer1* expression in the rudimentary foregut pocket. Lateral (E), anterior (F) and dorsal (G) views of early-somite stage wild type (E) and *Mixl1*$^{-/-}$ embryos (F,G) showing *Sox17* expression in the endoderm of the presumptive foregut (arrows in G,H) but not in the hindgut of the mutant embryo. (H) Transverse section at the plane shown in G.

Mixl1$^{-/-}$ embryo and the low contribution of the *Mixl1*$^{-/-}$ cells to the gut endoderm of the chimeras indicate that *Mixl1* function is essential for gut morphogenesis and the potency of the embryonic cells for endoderm differentiation. Members of the Mix/Bix family have been implicated in endoderm formation in both *Xenopus* and zebrafish. In the mouse, the definitive endoderm is formed by recruitment from the epiblast to the endodermal layer and replaces the visceral endoderm during gastrulation (Lawson et al., 1987; Lawson et al., 1991; Tremblay et al., 2000). In *Mixl1*$^{-/-}$ embryos, progenitors of definitive endoderm are properly specified at gastrulation. However, by the early somite stage, only a small population of presumptive definitive endodermal cells characterized by *Sox17* and *Cer1* expression is found in the poorly developed foregut portal. The reduction in definitive endoderm is consistent with the finding that fewer *Mixl1*$^{-/-}$ cells colonize the foregut and almost none are found in the hindgut of the chimera. *Mixl1*$^{-/-}$ cells can, however, colonize all other types of embryonic tissues, including the axial mesendoderm, neural tube and heart of the chimera. These results suggest that the abnormalities of gastrulation and organogenesis in the mutant embryo are probably caused by the disruption of the non-autonomous functions of *Mixl1*, but *Mixl1* plays a tissue-specific and autonomous role in the differentiation of embryonic cells into definitive endoderm. As *Mixl1* expression ceases in the definitive endoderm after its allocation to the embryonic gut, it is likely that *Mixl1* activity impacts on the endodermal progenitors while they are in the anterior primitive streak.

The *Mixl1* mutant phenotype points to a perturbation of signaling pathways regulating morphogenesis of mesendodermal tissues

Studies in *Xenopus* and zebrafish have shown that Mix/Bix genes are downstream transcriptional targets in the TGFβ superfamily pathway that regulates mesendodermal patterning. In the mouse embryo, the TGFβ family member *Nodal* is a key regulator of the formation of the anterior primitive streak, node, midline structures and definitive endoderm (reviewed by

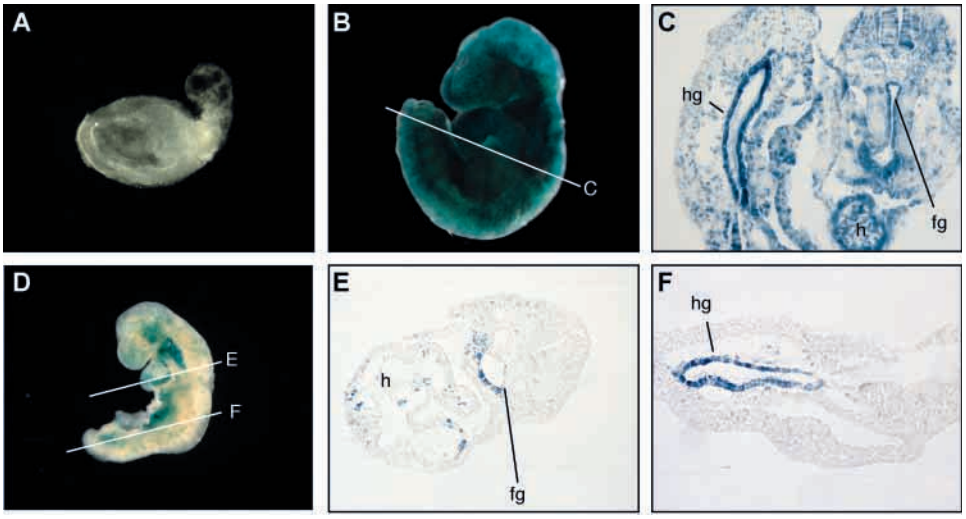

Fig. 9. *Mixl1*$^{-/-}$ ES cells (identified by the lack of *lacZ* activity) display reduced potency to colonize the embryonic endoderm. (A) A chimera with more than 90% contribution of *Mixl1*$^{-/-}$ ES cells recapitulates the phenotype of *Mixl1*$^{-/-}$ embryo. (B) A chimera with low *Mixl1*$^{-/-}$ ES cell contribution shows widespread distribution of the mutant cells in the embryonic tissue (C, plane of sectioning indicated in B), but poor contribution to the endoderm of the foregut (fg) and hindgut (hg). (D) A chimera with high mutant ES cell contribution shows extensive colonization of most embryonic tissues by the mutant cells, but sparse presence in the foregut endoderm (E) and complete absence from the hindgut endoderm (F). Planes of sectioning for E,F are indicated in D.

Schier and Shen, 2000). LEFTY2 (EGFB – Mouse Genome Informatics) is an atypical member of the TGFβ superfamily that antagonizes NODAL signaling and restricts the range and duration of NODAL activity (Meno et al., 1999; Meno et al., 2001). At gastrulation, *Lefty2* mutants, like *Mixl1* mutants, have an expanded primitive streak with an excess of axial mesoderm leading to a variety of associated patterning defects (Meno et al., 1999). In 7.5 dpc *Mixl1*$^{-/-}$ embryos, *Lefty2* expression in the primitive streak was unaltered (data not shown).

Nodal expression is expanded in the *Mixl1*$^{-/-}$ embryo, raising the possibility that *Mixl1* may to regulate NODAL activity. Ectopic expression studies in *Xenopus* and zebrafish embryos have shown that NODAL and related factors can induce the formation of mesoderm and axis duplication (Jones et al., 1995; Toyama et al., 1995; Joseph and Melton, 1997). In mouse chimeras, *Nodal*$^{-/-}$ cells are impaired in their ability to contribute to midline structures, indicating *Nodal* is required for midline morphogenesis (Varlet et al., 1997). Furthermore, *Smad2*, which is activated by *Nodal*, is required for definitive endoderm formation and embryos with a null mutation of the forkhead DNA-binding protein *Foxh1*, which binds *Smad2* (and *Smad3*), exhibit abnormal patterning of the node, prechordal mesoderm, notochord and definitive endoderm (Tremblay et al., 2000; Hoodless et al., 2001; Yamamoto et al., 2001). Taken together, these observations showing disruption of the morphogenesis of mesendodermal structures following alteration of NODAL signaling suggest that *Mixl1*, like its *Xenopus* homologs, may influence the spatial or temporal pattern of NODAL signaling in the mouse embryo.

Potential impact of *Mixl1* function on *Brachyury* activity

A role for the T-box gene *Brachyury* in notochord maintenance, axis elongation and specification of posterior mesoderm has been identified in many vertebrate species (Schulte-Merker et al., 1994; Wilson et al., 1995b; Conlon and Smith, 1999). In *Xenopus*, members of the Mix/Bix family have been shown to regulate expression of the *Brachyury* homolog *Xbra* (Latinkic et al., 1997; Tada et al., 1998; Casey et al., 1999; Latinkic and Smith, 1999). At the early gastrula stage, *Xbra* is expressed throughout the marginal zone of the embryo. In response to activin signaling, as gastrulation proceeds, transcripts are lost from involuting mesoderm, but persist in the notochord (Smith et al., 1991). *Mix.1*, which is induced by activin, downregulates *Xbra* transcription, in part through activation of *Gsc* (Artinger et al., 1997; Latinkic et al., 1997; Latinkic and Smith, 1999). In the *Mixl1*$^{-/-}$ embryos, the *Brachyury* expression domain is strikingly expanded in the primitive streak and also in the abnormal midline structures present in older mutants, with weaker activity in the condensed ‘core’ cells of the midline structure and of the primitive streak. This suggests that, like *Mix.1* in *Xenopus*, *Mixl1* may be acting as a repressor of *Brachyury* expression in the murine embryo.

Functional convergence of zebrafish and mammalian *Mix/Bix* family members

In zebrafish, the *Mix*-like gene, *Bon*, is responsible for the *bonnie and clyde* mutation (Kikuchi et al., 2000). Like *Mixl1*$^{-/-}$ embryos, *Bon* mutants have cardiac bifida and a reduction in *Sox17*-expressing endodermal cells. However, they do not show the drastic disruption in axial morphogenesis seen in *Mixl1*-null embryos. Within the homeodomain, MIXL1 is more closely related to BON than any member of the *Xenopus* MIX/BIX family. Nevertheless, given that the overall the amino acid identity of BON and MIXL1 is only 25% and, taken together with the differences in phenotype of *Bon* and *Mixl1* mutants, it is likely that the zebrafish homolog of *Mixl1* remains to be discovered. *Mixl1* is the only known mammalian member of the Mix/Bix family, and searching of the mouse and human genomes has not uncovered other potential homologs (A. H. H., A. G. E. and L. R., unpublished). By contrast, in *Xenopus*, seven *Mix*-like genes may be involved in the transcriptional regulation of mesoderm and endoderm development. Our study shows that, in the mouse, *Mixl1* serves many functions of the *Xenopus* Mix/Bix genes to control the morphogenesis of mesendodermal structures, especially the node, notochord, axial mesoderm and the gut, and the differentiation of the definitive endoderm. We postulate that *Mixl1* is the functional mammalian homolog of the members of the *Xenopus* Mix/Bix homeodomain family.

We are grateful to Peter Gruss, Hiroshi Hamada, Elizabeth Jones, Richard Harvey, Bernhard Herrmann, Gail Martin, Andrew McMahon, Virginia Papaioannou, Janet Rossant, Bill Shawlot Miles Wilkinson and Chris Wright for the provision of riboprobes; to Liz Robertson for generously providing R26.1 ES cells and *Nodal*$^{+/lacZ}$ mice; to Steven Mihajlovic for assistance with histology; to Dennis Advani for the preparation of illustrations; to Bette Borobakas, Marilyn Ibrahim and Anita Steptoe for expert technical assistance; and to Peter Rowe for reading the manuscript. The project was supported by the National Health and Medical Research Council of Australia, the Cooperative Research Centre for Cellular Growth Factors, The Sylvia and Charles Viertel Charitable Foundation and the Anti-Cancer Council of Victoria. L. R. is a Viertel Foundation Senior Research Fellow, A. G. E. is an NHMRC Senior Research Fellow and P. P. L. T. is a NHMRC Senior Principal Research Fellow.

REFERENCES

Alexander, J. and Stainier, D. Y. R. (1999). A molecular pathway leading to endoderm formation in zebrafish. *Curr. Biol.* **9**, 1147-1157.

Alexander, J., Rothenberg, M., Henry, G. L. and Stainier, D. Y. R. (1999). *casanova* plays an early and essential role in endoderm formation in zebrafish. *Dev. Biol.* **215**, 343-357.

Ang, S. L., Wierda, A., Wong, D., Stevens, K. A., Cascio, S., Rossant, J. and Zaret, K. S. (1993). The formation and maintenance of the definitive endoderm lineage in the mouse: involvement of HNF3/forkhead proteins. *Development* **119**, 1301-1315.

Artinger, M., Blitz, I., Inoue, K., Tran, U. and Cho, K. W. (1997). Interaction of goosecoid and brachyury in Xenopus mesoderm patterning. *Mech. Dev.* **65**, 187-196.

Beddington, R. S. and Robertson, E. J. (1989). An assessment of the developmental potential of embryonic stem cells in the mid gestational mouse embryo. *Development* **105**, 733-737.

Belo, J. A., Bouwmeester, T., Leyns, L., Kertesz, N., Gallo, M., Follettie, M. and de Robertis, E. M. (1997). Cerberus-like is a secreted factor with neutralizing activity expressed in the anterior primitive endoderm of the mouse gastrula. *Mech. Dev.* **68**, 45-57.

Biben, C., Stanley, E., Fabri, L., Kotecha, S., Rhinn, M., Drinkwater, C., Lah, M., Wang, C. C., Nash, A., Hilton, D., Ang, S. L., Mohun, T. and Harvey, R. P. (1998). Murine cerberus homologue mCer-1: a candidate anterior patterning molecule. *Dev. Biol.* **194**, 135-151.

Casey, E. S., Tada, M., Fairclough, L., Wylie, C. C., Heasman, J. and Smith, J. C. (1999). Bix4 is activated directly by VegT and mediates endoderm formation in Xenopus development. *Development* **126**, 4193-4200.

Collignon, J., Varlet, I. and Robertson, E. J. (1996). Relationship between

asymmetric nodal expression and the direction of embryonic turning. *Nature* **381**, 155-158.

Conlon, F. L., Lyons, K. M., Takaesu, N., Barth, K. S., Kispert, A., Herrmann, B. and Robertson, E. J. (1994). A primary requirement for nodal in the formation and maintenance of the primitive streak in the mouse. *Development* **120**, 1919-1928.

Conlon, F. L. and Smith, J. C. (1999). Interference with brachyury function inhibits convergent extension, causes apoptosis, and reveals separate requirements in the FGF and activin signalling pathways. *Dev. Biol.* **213**, 85-100.

Dziadek, M. and Adamson, E. (1978). Localization and synthesis of alphafoetoprotein in post-implantation mouse embryos. *J. Embryol. Exp. Morphol.* **43**, 289-313.

Echelard, Y., Epstein, D. J., St-Jacques, B., Shen, L., Mohler, J., McMahon, J. A. and McMahon, A. P. (1993). Sonic hedgehog, a member of a family of putative signaling molecules, is implicated in the regulation of CNS polarity. *Cell* **75**, 1417-1430.

Ecochard, V., Cayrol, C., Rey, S., Foulquier, F., Caillol, D., Lemaire, P. and Duprat, A. M. (1998). A novel Xenopus mix-like gene milk involved in the control of the endomesodermal fates. *Development* **125**, 2577-2585.

Elefanty, A. G., Begley, C. G., Hartley, L., Papaevangeliou, B. and Robb, L. (1999). SCL expression in the mouse embryo detected with a targeted lacZ reporter gene demonstrates its localization to hematopoietic, vascular, and neural tissues. *Blood* **94**, 3754-3763.

Friedrich, G. and Soriano, P. (1991). Promoter traps in embryonic stem cells: a genetic screen to identify and mutate developmental genes in mice. *Genes Dev.* **5**, 1513-1523.

Germain, S., Howell, M., Esslemont, G. M. and Hill, C. S. (2000). Homeodomain and winged-helix transription factors recruit activated Smads to distinct promoter elements via a common Smad interaction motif. *Genes Dev.* **14**, 435-451.

Godwin, A. R., Stadler, H. S., Nakamura, K. and Capecchi, M. R. (1998). Detection of targeted GFP-Hox gene fusions during mouse embryogenesis. *Proc. Natl. Acad. Sci. USA* **95**, 13042-13047.

Henry, G. L. and Melton, D. A. (1998). Mixer, a homeobox gene required for endoderm development. *Science* **281**, 91-96.

Hoodless, P. A., Pye, M., Chazaud, C., Labbe, E., Attisano, L., Rossant, J. and Wrana, J. L. (2001). FoxH1 (Fast) functions to specify the anterior primitive streak in the. *Genes Dev.* **15**, 1257-1271.

Hudson, C., Clements, D., Friday, R. V., Stott, D. and Woodland, H. R. (1997). Xsox17alpha and beta mediate endoderm formation in Xenopus. *Cell* **91**, 397-405.

Jones, C. M., Kuehn, M. R., Hogan, B. L., Smith, J. C. and Wright, C. V. (1995). Nodal-related signals induce axial mesoderm and dorsalize mesoderm during gastrulation. *Development* **121**, 3651-3662.

Joseph, E. M. and Melton, D. A. (1997). Xnr4: a Xenopus nodal-related gene expressed in the Spemann organizer. *Dev. Biol.* **184**, 367-372.

Kanai-Azuma, M., Kanai, Y., Gad, J. M., Tajima, Y., Taya, C., Kurohmaru, M., Sanai, Y., Yonekawa, H., Yazaki, K., Tam, P. P. L. and Hayashi, Y. (2002). Depletion of definitive gut endoderm in *Sox17*-null mutant mice. *Development* **129**, 2367-2379.

Kikuchi, Y., Trinh, L. A., Reiter, J. F., Alexander, J., Yelon, D. and Stainer, D. Y. R. (2000). The zebrafish bonnie and clyde gene encodes a Mix family homeodomain protein that regulates the generation of endodermal precursors. *Genes Dev.* **14**, 1279-1289.

Kinder, S. J., Tsang, T. E., Ang, S. L., Behringer, R. R. and Tam, P. P. (2001). Defects of the body plan of mutant embryos lacking Lim1, Otx2 or Hnf3beta activity. *Int. J. Dev. Biol.* **45**, 347-355.

Latinkic, B. V. and Smith, J. C. (1999). Goosecoid and mix.1 repress Brachyury expression and are required for head formation in Xenopus. *Development* **126**, 1769-1779.

Latinkic, B. V., Umbhauer, M., Neal, K. A., Lerchner, W., Smith, J. C. and Cunliffe, V. (1997). The Xenopus Brachyury promoter is activated by FGF and low concentrations of activin and suppressed by high concentrations of activin and by paired-type homeodomain proteins. *Genes Dev.* **11**, 3265-3276.

Lawson, K. A. and Pedersen, R. A. (1987). Cell fate, morphogenetic movement and population kinetics of embryonic endoderm at the time of germ layer formation in the mouse. *Development* **101**, 627-652.

Lawson, K. A., Meneses, J. J. and Pedersen, R. A. (1991). Clonal analysis of epiblast fate during germ layer formation in the mouse embryo. *Development* **113**, 891-911.

Lemaire, P., Darras, S., Caillol, D. and Kodjabachian, L. (1998). A role for the vegetally expressed Xenopus gene Mix.1 in endoderm formation and in the restriction of mesoderm to the marginal zone. *Development* **125**, 2371-2380.

Lin, T. P., Labosky, P. A., Grabel, L. B., Kozak, C. A., Pitman, J. L., Kleeman, J. and MacLeod, C. L. (1994). The Pem homeobox gene is X-linked and exclusively expressed in extraembryonic tissues during early murine development. *Dev. Biol.* **166**, 170-179.

Lyons, I., Parsons, L., Hartley, L., Li, R., Andrews, J., Robb, L. and Harvey, R. P. (1995). Myogenic and morphogenetic defects in the heart tubes of murine embryos lacking the homeobox gene *Nkx2-5*. *Genes Dev.* **9**, 1654-1666.

Massague, J. and Wotton, D. (2000). Transcriptional control by the TGF-beta/Smad signaling system. *EMBO J.* **19**, 1745-1754.

Mead, P. E., Brivanlou, I. H., Kelley, C. M. and Zon, L. I. (1996). BMP-4-responsive regulation of dorsal-ventral patterning by the homeobox protein Mix.1. *Nature* **382**, 357-360.

Mead, P. E., Zhou, Y., Lustig, K. D., Huber, T. L., Kirschner, M. W. and Zon, L. I. (1998). Cloning of Mix-related homeodomain proteins using fast retrieval of gel shift activities, (FROGS), a technique for the isolation of DNA-binding proteins. *Proc. Natl. Acad. Sci. USA* **95**, 11251-11256.

Meno, C., Gritsman, K., Ohishi, S., Ohfuji, Y., Heckscher, E., Mochida, K., Shimono, A., Kondoh, H., Talbot, W. S., Robertson, E. J., Schier, A. F. and Hamada, H. (1999). Mouse Lefty2 and zebrafish antivin are feedback inhibitors of nodal signaling during vertebrate gastrulation. *Mol. Cell* **4**, 287-298.

Meno, C., Takeuchi, J., Sakuma, R., Koshiba-Takeuchi, K., Ohishi, S., Saijoh, Y., Miyazaki, J., ten Dijke, P., Ogura, T. and Hamada, H. (2001). Diffusion of nodal signaling activity in the absence of the feedback inhibitor Lefty2. *Dev. Cell* **1**, 127-138.

Moens, C. B., Stanton, B. R., Parada, L. F. and Rossant, J. (1993). Defects in heart and lung development in compound heterozygotes for two different targeted mutations at the N-myc locus. *Development* **119**, 485-499.

Monaghan, A. P., Kaestner, K. H., Grau, E. and Schutz, G. (1993). Postimplantation expression patterns indicate a role for the mouse forkhead/HNF-3 alpha, beta and gamma genes in determination of the definitive endoderm, chordamesoderm and neuroectoderm. *Development* **119**, 567-578.

Oliver, G., Mailhos, A., Wehr, R., Copeland, N. G., Jenkins, N. A. and Gruss, P. (1995). Six3, a murine homologue of the sine oculis gene, demarcates the most anterior border of the developing neural plate and is expressed during eye development. *Development* **121**, 4045-4055.

Peale, F. V., Jr, Sugden, L. and Bothwell, M. (1998). Characterization of CMIX, a chicken homeobox gene related to the Xenopus gene mix.1. *Mech. Dev.* **75**, 167-170.

Pearce, J. J. and Evans, M. J. (1999). Mml, a mouse mix-like gene expressed in the primitive streak. *Mech. Dev.* **87**, 189-192.

Robb, L., Lyons, I., Li, R., Hartley, L., Harvey, R. P., Kontgen, F. and Begley, C. G. (1995). Absence of yolk sac hematopoiesis from mice with a targeted disruption of the *scl* gene. *Proc. Natl. Acad. Sci. USA* **92**, 7075-7079.

Robb, L., Hartley, L., Begley, C. G., Brodnicki, T. C., Copeland, N. G., Gilbert, D. J., Jenkins, N. A. and Elefanty, A. G. (2000). Cloning, expression analysis, and chromosomal localization of murine and human homologues of a Xenopus mix gene. *Dev. Dyn.* **219**, 497-504.

Roelink, H., Augsburger, A., Heemskerk, J., Korzh, V., Norlin, S., Ruiz i Altaba, A., Tanabe, Y., Placzek, M., Edlund, T., Jessell, T. M. et al. (1994). Floor plate and motor neuron induction by vhh-1, a vertebrate homolog of hedgehog expressed by the notochord. *Cell* **76**, 761-775.

Rosa, F. M. (1989). Mix.1, a homeobox mRNA inducible by mesoderm inducers, is expressed mostly in the presumptive endodermal cells of Xenopus embryos. *Cell* **57**, 965-974.

Ruiz i Altaba, A., Prezioso, V. R., Darnell, J. E. and Jessell, T. M. (1993). Sequential expression of HNF-3 beta and HNF-3 alpha by embryonic organizing centers: the dorsal lip/node, notochord and floor plate. *Mech. Dev.* **44**, 91-108.

Sasaki, H. and Hogan, B. L. (1993). Differential expression of multiple fork head related genes during gastrulation and axial pattern formation in the mouse embryo. *Development* **118**, 47-59.

Schier, A. F. and Shen, M. M. (2000). Nodal signalling in vertebrate development. *Nature* **403**, 385-389.

Schulte-Merker, S., van Eeden, F. J., Halpern, M. E., Kimmel, C. B. and Nusslein-Volhard, C. (1994). no tail (ntl) is the zebrafish homologue of the mouse T (Brachyury) gene. *Development* **120**, 1009-1015.

Schwenk, F., Baron, U. and Rajewsky, K. (1995). A cre-transgenic mouse

strain for the ubiquitous deletion of loxP-flanked gene segments including deletion in germ cells. *Nucleic Acids Res.* **23**, 5080-5081.

Shawlot, W., Deng, J. M. and Behringer, R. R. (1998). Expression of the mouse cerberus-related gene, Cerr1, suggests a role in anterior neural induction and somitogenesis. *Proc. Natl. Acad. Sci. USA* **95**, 6198-6203.

Simeone, A., Acampora, D., Mallamaci, A., Stornaiuolo, A., D'Apice, M. R., Nigro, V. and Boncinelli, E. (1993). A vertebrate gene related to orthodenticle contains a homeodomain of the bicoid class and demarcates anterior neuroectoderm in the gastrulating mouse embryo. *EMBO J.* **12**, 2735-2747.

Smith, J. C., Price, B. M., Green, J. B., Weigel, D. and Herrmann, B. G. (1991). Expression of a Xenopus homolog of Brachyury (T) is an immediate-early response to mesoderm induction. *Cell* **67**, 79-87.

Stein, S., Roeser, T. and Kessel, M. (1998). CMIX, a paired-type homeobox gene expressed before and during formation of the avian primitive streak. *Mech. Dev.* **75**, 163-165.

Tada, M., Casey, E. S., Fairclough, L. and Smith, J. C. (1998). Bix1, a direct target of Xenopus T-box genes, causes formation of ventral mesoderm and endoderm. *Development* **125**, 3997-4006.

Toyama, R., O'Connell, M. L., Wright, C. V., Kuehn, M. R. and Dawid, I. B. (1995). Nodal induces ectopic goosecoid and lim1 expression and axis duplication in zebrafish. *Development* **121**, 383-391.

Tremblay, K. D., Hoodless, P. A., Bikoff, E. K. and Robertson, E. J. (2000). Formation of the definitive endoderm in mouse is a Smad2-dependent. *Development* **127**, 3079-3090.

Varlet, I., Collignon, J. and Robertson, E. J. (1997). nodal expression in the primitive endoderm is required for specification of the anterior axis during mouse gastrulation. *Development* **124**, 1033-1044.

Vize, P. D. (1996). DNA sequences mediating the transcriptional response of the Mix.2 homeobox gene to mesoderm induction. *Dev. Biol.* **177**, 226-231.

Wilkinson, D. G., Bhatt, S. and Herrmann, B. G. (1990). Expression pattern of the mouse T gene and its role in mesoderm formation. *Nature* **343**, 657-659.

Wilson, D., Sheng, G., Lecuit, T., Dostatni, N. and Desplan, C. (1993). Cooperative dimerization of paired class homeo domains on DNA. *Genes Dev.* **7**, 2120-2134.

Wilson, D. S., Guenther, B., Desplan, C. and Kuriyan, J. (1995a). High resolution crystal structure of a paired (Pax) class cooperative homeodomain dimer on DNA. *Cell* **82**, 709-719.

Wilson, V., Manson, L., Skarnes, W. C. and Beddington, R. S. (1995b). The T gene is necessary for normal mesodermal morphogenetic cell movements during gastrulation. *Development* **121**, 877-886.

Xanthos, J. B., Kofron, M., Wylie, C. and Heasman, J. (2001). Maternal VegT is the initiator of a molecular network specifying endoderm in Xenopus laevis. *Development* **128**, 167-180.

Yamamoto, M., Meno, C., Sakai, Y., Shiratori, H., Mochida, K., Ikawa, Y., Saijoh, Y. and Hamada, H. (2001). The transcription factor FoxH1 (FAST) mediates Nodal signaling during anterior-posterior patterning and node formation in the mouse. *Genes Dev.* **15**, 1242-1256.

Zhou, X., Sasaki, H., Lowe, L., Hogan, B. L. and Kuehn, M. R. (1993). Nodal is a novel TGF-beta-like gene expressed in the mouse node during gastrulation. *Nature* **361**, 543-547.